Structures of the Clusters Produced by Laser Desorption of Fullerenes: [2+2] Cycloadducts of Preshrunk Cages

Alexandre A. Shvartsburg, Lisa A. Pederson, Robert R. Hudgins, George C. Schatz,* and Martin F. Jarrold*

Department of Chemistry, Northwestern University, 2145 Sheridan Road, Evanston, Illinois 60208

The laser desorption of C_{60} or C_{70} fullerenes yields a distribution of ions with masses corresponding to an even number of carbon atoms around integer multiples of 60 or 70. Clusters with 120 or 140 atoms have been characterized as large coalesced fullerenes and fullerene dimers joined by a [2+2] cycloaddition. Several structures had been proposed for the species with less than an integer multiple of 60 or 70 atoms, but none of them has been validated experimentally. We have examined C_n (n = 112, 114, 116, 118, 136, and 138) cations and anions using high resolution ion mobility measurements and compared the results with trajectory calculations for a number of candidate geometries. We find that these species exist as near-spherical cages and [2+2] cycloadducts of smaller fullerenes derived from C_{60} or C_{70}. Quadruply bound C_{116}, C_{118}, C_{136}, and C_{138} isomers that would result from the stepwise elimination of C_2 from the preformed [2+2] C_{60} or C_{70} dimers were not observed. Hence the fullerene dimers lacking a few atoms are formed by coalescence of dissociation products rather than by dissociation of the products of coalescence. Plausible reasons why the [2+2] cycloadducts are the only dimers produced by the laser desorption of fullerenes are discussed.

Introduction

Soon after the C_{60} fullerene was isolated, experiments on its laser desorption were performed. The abundance of desorbed ions peaks strongly in the vicinity of 720k amu, indicating the accretion of fullerenes upon laser desorption.[1−14] Analogous observations for the C_{70} films have been reported.[9,15−17] The structure of resulting products has been a subject of discussion, with indirect arguments in favor of either complete coalescence into giant single-shell fullerenes[1,3] or polymerization by cross-linking individual C_{60} cages.[5−11] Hunter et al.[18] have shown using ion mobility measurements that for C_{120} cation both types of species could be synthesized, depending on conditions. We have recently taken advantage of a new high resolution ion mobility apparatus[19] to elucidate the structures of these two products as a near-spherical fullerene and a [2+2] cycloadduct (Figure 1) for both C_{120} cations and anions.[20] The results for $C_{130}^{+/−}$ and $C_{140}^{+/−}$ clusters were similar.[20] Prior to our work, there were already calculations and indirect experimental evidence from the solid state research suggesting that the C_{60} dimer is bound by the [2+2] cycloaddition links (see citations in ref 20). New theoretical[17,21−27] and experimental[8,28−41] studies have further strengthened that assignment. The final confirmation has recently come from the Komatsu[42] and Kratschmer[43] groups which have isolated the C_{60} dimer in bulk and probed it using NMR, IR, X-ray,[42] and Raman spectroscopies.[43]

However, the abundance maxima in the laser desorption mass spectra usually occur not at 60k carbons, but at slightly lower masses[1−7,9,11−14] in the range of 59k to 55k. For C_{70}, the mass spectrum has its maximum[9,15,17] at 68k or 67k. It has been suggested[11,17] that these maxima correspond to particularly stable clusters in the sequence produced by the stepwise dissociation of $(C_{60})_k$ or $(C_{70})_k$ oligomers. Using dimers as models and employing semiempirical AM1 and PM3 methods, Ata et al.[11,17] have investigated a number of "dumbbell" isomers for C_{118},
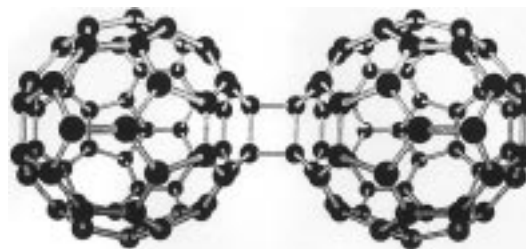

Figure 1. The C_{60} dimer, a [2+2] cycloadduct.

C_{116}, C_{138}, and C_{136} with different links between the cages. In particular, quadruply bound "ladder" geometries for C_{118} and C_{116} have larger cohesive energies than the $(C_{60})_2$ [2+2] cycloadduct.[11] The C_{118} species (Figure 2a) was postulated[11,17] to be produced from [2+2] $(C_{60})_2$ (Figure 1) via (i) scission of two opposing hinge bonds forming the four-membered ring, (ii) Stone-Wales (fulvalene−napthalene) rearrangement[44,45,46] of both linking pivot bonds yielding a quadruply bound C_{60} dimer, and (iii) elimination of a C_2 unit from one of the two equivalent bridges. A similar loss of C_2 from the other bridge would then result in the C_{116} (Figure 2b). It has been suggested[11,17] that this C_{116} D_{2h} structure and the homologous one derived from a [2+2] C_{70} dimer are responsible for the C_{116} and C_{136} peaks in the mass spectra.

However, the pathways of sequential C_2 elimination that were postulated[11,17] to lead from a [2+2] $(C_{60})_2$ to the C_{118} and C_{116} species considered in ref 11 (or from $(C_{70})_2$ to C_{138} and C_{136} in ref 17) are thermodynamically implausible, even if reasonable from a purely mechanistic viewpoint. This is because the experimental activation barriers for the competing processes of dissociation of a [2+2] cycloadduct back to C_{60} monomers or its isomerization into a single large C_{120} cage are about 1.5 eV in both cases.[18,47] This energy is much less than that required to eliminate a C_2 unit from a fullerene network. At the AM1 level, ∼7.5 eV would be needed to eliminate C_2 from the [2+2]
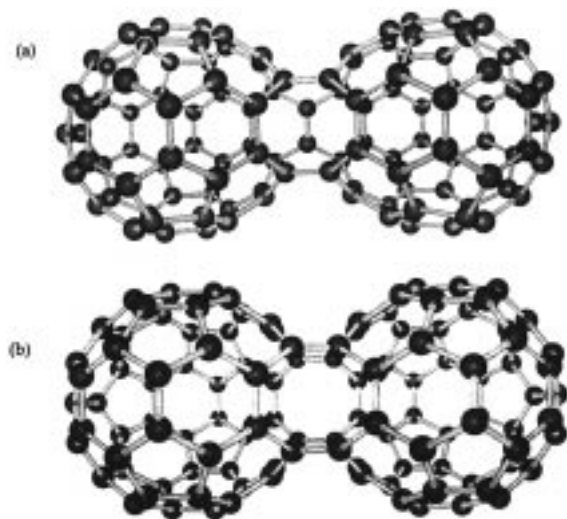
Figure 2. Previously proposed[11] quadruply bound dimer structures C_{118} (a) and C_{116} D_{2h} (b).

$(C_{60})_2$ and produce the C_{118} structure in Figure 2a, even if the reverse association reaction had no activation barrier. In fact, C_{120} should not evaporate C_2 until isomerization into a large cage is complete. Hence it is highly unlikely that any dumbbell-shaped carbon clusters with less than 120 atoms could be produced in any abundance by heating a C_{60} dimer. C_{60} has a triplet state with a lifetime of 42 us at 1.7 eV above the ground state.[48] This triplet state could play a role in the [2+2] cycloaddition. However, the electronic energy of this state is insufficient to promote C_2 loss from the [2+2] dimer. The same holds for C_{70}.[48]

Contrary to the above picture, where dimerization occurs prior to dissociation, Hertel and collaborators[13] speculated that the C_{120-2k} peaks observed in the laser desorption mass spectra of C_{60} are simply the coalescence products of cages that had already undergone one or more steps of the C_2 loss: the "shrinking" process normally occurring upon heating gas phase fullerenes. This would explain why the position of maximum cluster abundance varies among different groups and shifts to smaller masses with increasing laser fluence.[5,13,14] As the $(C_{60})_2$, $C_{60} \cdot C_{70}$ and $(C_{70})_2$ are all [2+2] cycloadducts,[20] one may expect the dimers of other fullerenes in this size range to be the same. On the other hand, these other fullerenes do not follow the isolated pentagon rule (IPR), and thus they have special sites with two or more abutting pentagons. These sites substantially augment the reactivity of C_{56} and C_{58} cations as compared to C_{60},[49] and they might affect the structure of dimers incorporating such cages. In order to test the contradicting propositions for the structure of fullerene coalescence products, we have measured the gas phase mobilities of C_n cations and anions for $n = 112-120$ and $n = 136-140$ (*n* even).

Experimental Methods

The experiments were performed on our high resolution ion mobility apparatus described in detail elsewhere.[19] All the conditions and procedures were identical to those employed in our previous study of the fullerene dimers,[20] except that the laser power was increased in order to enhance the abundance of clusters other than those with $n = 120$ and 140. Briefly, the clusters are generated by pulsed 308 nm laser desorption of a fullerene film deposited on a copper rod. The ions thus formed are directed by shaped electric fields through an ion gate into a drift tube filled with helium buffer gas at a pressure of around 500 Torr. The ions then travel along the length of the drift tube under the influence of a uniform electric field created by a stack of isolated rings and a voltage divider. Species exiting through a small aperture at the end of drift tube are mass selected by a quadrupole mass spectrometer and detected by an off-axis collision dynode and dual microchannel plates. Arrival time distributions are recorded with a multichannel scaler using the laser pulse as the start trigger. The measured drift time, t_d is converted into a mobility via the relationship[50] $K = L^2/(t_d V)$, where L is the length of drift tube and V is the voltage drop across it. All measurements were performed at the temperature of 25 °C. Two different film samples were used: purified C_{60} (Bucky USA) and a C_{60}/C_{70} mixture. The former obviously would not yield mass peaks close to $n = 140$. However, the results for clusters with $n = 112-120$ produced from the two samples are indistinguishable.

Results

The drift time distributions measured for C_{116}^+, C_{118}^+, C_{136}^+, and C_{138}^+ are presented in Figure 3. The scans obtained for the corresponding anions, and for both cations and anions of C_{112} and C_{114} are very similar. Scales on the top of figures indicate the inverse reduced mobilities. This has become a customary way to express ion mobility data because the inverse mobilities are proportional to the orientationally averaged collision integrals.[50] The distributions for all six cluster sizes closely resemble those reported for C_{120}, C_{130}, and C_{140} ions.[19] Namely, (i) there are two fully resolved features that correspond to a closed cage fullerene and a dimer; (ii) the fullerene peaks are broader than those expected for a single isomer, with asymmetric tails that extend to longer drift times; and (iii) with increasing laser power, the dimer peaks decrease relative to the fullerene peaks, which narrow and shift to slightly shorter drift times corresponding to the fullerenes produced by laser vaporization of graphite.

Mobility Calculations. In the low field limit where all our experiments are performed, the mobility is independent of the drift field and given by[50]

$$K = \frac{(18\pi)^{1/2}}{16} \left[\frac{1}{m} + \frac{1}{m_b} \right]^{1/2} \frac{ze}{k_B T^{1/2}} \frac{1}{\Omega_{avg}^{(1,1)}} \frac{1}{N} \quad (1)$$

where m and m_b are respectively the masses of the ion and of the buffer gas atom, N is the buffer gas number density, T is the gas temperature, ze is the ionic charge, and $\Omega_{avg}^{(1,1)}$ is the orientationally averaged collision integral (cross section).

We determine the $\Omega_{avg}^{(1,1)}$ for candidate geometries in two ways. In the more rigorous approach, classical trajectories for He atom/cluster collisions are propagated in a realistic intermolecular potential.[51] Averaging a function of the scattering angle over the impact parameter and collision geometry yields the momentum transfer cross section. $\Omega_{avg}^{(1,1)}$ is evaluated by numerical integration of this cross section over the relative velocity distribution. The potential between the ion and buffer gas atoms is assumed to be given by a sum of pairwise Lennard-Jones interactions plus a charge-induced dipole term where the ionic charge is uniformly delocalized over all cluster atoms. The Lennard-Jones parameters for this potential ($\epsilon = 1.34$ meV and $\sigma = 3.043$ Å, where ϵ is the depth and σ is the distance where the potential energy is zero) were obtained by fitting the mobility of C_{60}^+ fullerene measured over an 80−400 K temperature range.[20,51] For each geometry, about 10^6 trajectories were propagated, which provides a statistical sampling error below 0.2%. The capability of this model to provide extremely
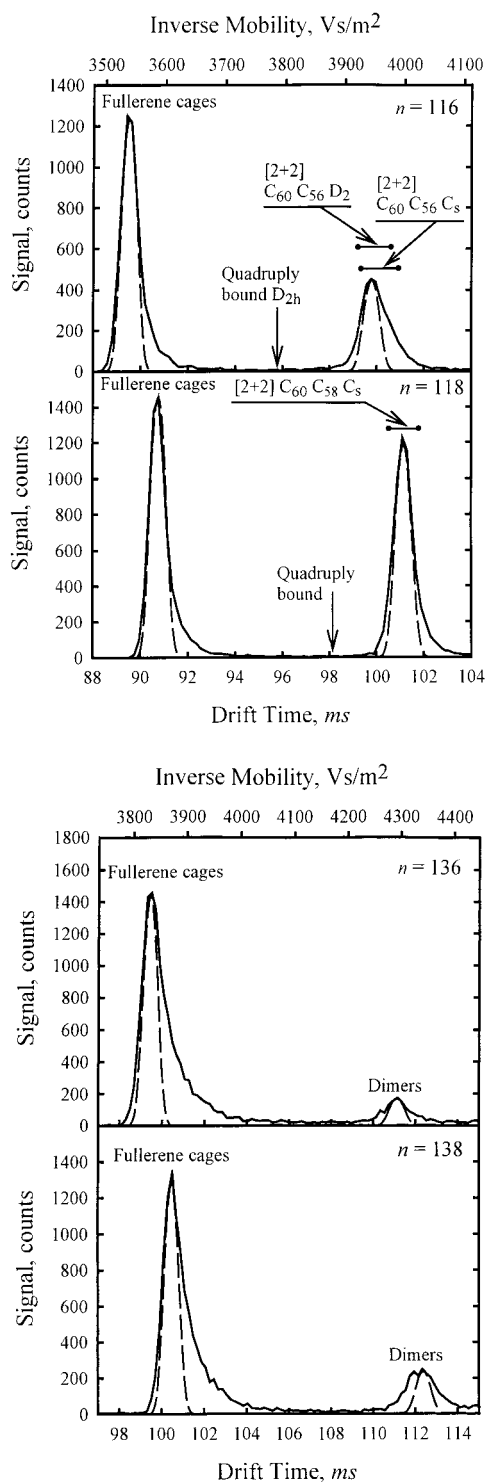
Figure 3. Drift time distributions measured for C_{116}^+ and C_{118}^+ (a), C_{136}^+ and C_{138}^+ (b) from the laser desorption of a fullerene film. The drift times computed for candidate geometries described in the text are superimposed in (a). The dashed lines show the ideal peak widths calculated for a single isomer. (Peaks would always have a finite width due to the diffusional broadening of ion packets in drift tube.)

accurate values for the mobilities of fullerenes and their dimers has already been demonstrated.[20,41] Now that the [2+2] structure for the $(C_{60})_2$ has been established, we use this dimer as a standard to achieve a still greater accuracy in mobility calculations for other fullerene dimers.

Trajectory calculations were performed for all species considered below except for the C_{116} and C_{118} geometries that we optimized. Unfortunately, the number of these isomers has

compelled us to evaluate their mobilities using a less computationally expensive method. The exact hard-spheres scattering (EHSS) model[52] which assumes a hard-sphere potential between buffer gas atoms and each cluster atom has been found[20] to systematically underestimate the collision integrals for the [2+2] cycloadducts of C_{60} by ~0.3% compared to the values from trajectory calculations. This allowed us to determine the mobilities for the dimers containing C_{56} and C_{58} using the EHSS model and correct the resulting values by 1.003.

Cluster Geometries. A large number of trial structures for "dimer" isomers of $n = 116$ and 118 were constructed by optimizing various [2+2] cycloadducts of C_{60} with C_{58} for C_{118}, and C_{60} with C_{56} and C_{58} with C_{58} for C_{116}. The semiempirical method AM1, which produces a $(C_{60})_2$ geometry in good agreement with experiment,[42] was used. The lowest energy isomer for $n = 58$ is C_s, but there are two nearly degenerate cages for $n = 56$: C_s and D_2.[53-55] However, the mobilities evaluated for the latter two are within 0.5% from each other. For both sizes, the agreement with the measurements for cations[56] is perfect: 2210 ± 10 Vs/m² versus 2210 ± 20 Vs/m² (experiment) for C_{56} and 2260 ± 5 Vs/m² versus 2260 ± 20 Vs/m² (experiment) for C_{58}.

There are 84 C–C bonds in C_{56} cages, out of which 46 are symmetry distinct in the C_s isomer and 22 are in the D_2 isomer. Out of 87 bonds in C_{58} C_s, 47 are unique. In principle, each of the unique bonds in these cages can form a four-membered ring in a [2+2] cycloadduct with either a hexagon-hexagon or a pentagon–hexagon bond in C_{60}. Since, in general, the rotation of one cage around the center-to-center axis by π results in a different molecule, hundreds of distinct $C_{60} \cdot C_{58}$ or $C_{60} \cdot C_{56}$ [2+2] cycloadducts (not including the enantiomers) could be assembled from even the lowest energy isomers of C_{58} or C_{56}. There are thousands of [2+2] $(C_{58})_2$ geometries. It is obviously not feasible to consider every imaginable combination. It is, however, reasonable to expect that the C–C bonds that are "double" in nature would be, by far, more reactive to the [2+2] cycloaddition. This has been the experience with C_{60} and C_{70}.[17] Hence we optimized the dimers built on a double (shared by two hexagons) bond for C_{60} and one of the shorter bonds or a bond in a non-IPR site for C_{56} and C_{58}. Overall, 18 distinct dimers were considered for $C_{60} \cdot C_{58}$ C_s, 16 for $C_{60} \cdot C_{56}$ D_2, and 21 for $C_{60} \cdot C_{56}$ C_s. Representatives for each of these three families are shown in Figure 4. As the C_{58} and both C_{56} cages are distorted from spherical, the mobilities calculated for clusters within each of the three families above change, depending on whether the attachment of C_{60} occurs at the "equatorial" or "polar" region, by about 1.0–1.5%, a value comparable with our experimental peak widths. However, the ranges for $C_{60} \cdot C_{58}$ C_s and $C_{60} \cdot C_{56}$ D_2 overlap significantly.

Structural Assignments. Mobilities calculated for our optimized [2+2] cycloadducts and for quadruply bound isomers previously proposed[11] for C_{116} and C_{118} (see Figure 2) are marked in the Figure 3. For both sizes, the [2+2] geometries are the only ones consistent with the experimental data. One could arrive at this conclusion even without optimizing any trial structures or performing any mobility calculations. In Figure 5, the mobilities measured for both the fullerene dimer and cage isomers in the $n = 112-140$ range are plotted as a function of n. By inspection, all dimers belong to a single structural family, which must be the [2+2] cycloadducts because that is the structure of $(C_{60})_2$.[42,43] In this way, we determine that the dimer isomers of C_{112}, C_{114}, C_{136}, and C_{138} are also formed by [2+2]
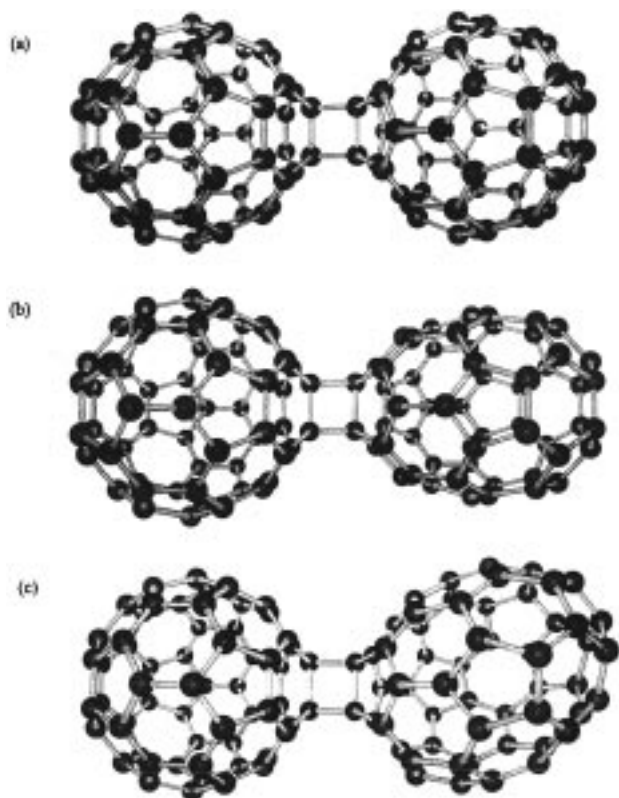
Figure 4. Examples of the optimized [2+2] cycloadducts: (a) $C_{60}\cdot C_{58}$ C_s, (b) $C_{60}\cdot C_{56}$ C_s, and (c) $C_{60}\cdot C_{56}$ D_2.
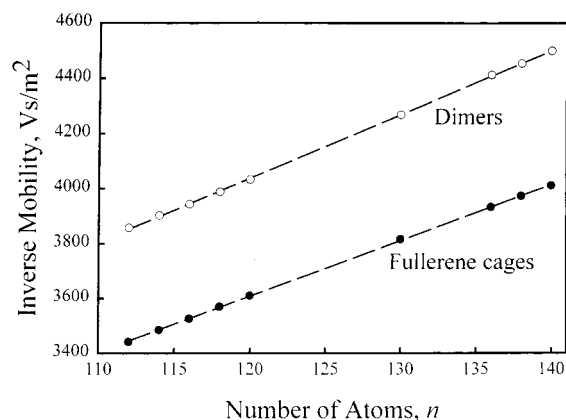
Figure 5. Inverse mobilities (reduced mobilities^{-1}) measured for the fullerene cage (●) and dimer (○) isomers. Lines are the first-order regressions through each sequence.

cycloaddition. It is interesting that, despite a rapid increase in the total number of structural possibilities in the progressions from $n = 120$ to $n = 112$ ($C_{60}\cdot C_{58}$ for C_{118}; $C_{60}\cdot C_{56}$ C_s, $C_{60}\cdot C_{56}$ D_2, and $C_{58}\cdot C_{56}$ for C_{116}, etc.) and similarly from $n = 140$ to $n = 136$, the measured width of the peaks hardly changes.

Figure 5 also reveals that, for fullerene cages with $112-118$, 136, or 138 atoms, the dominant isomers are clearly homologous to those of $C_{120}^{+/-}$, $C_{130}^{+/-}$, and $C_{140}^{+/-}$, and hence, they are also near-spherical in shape rather than elongated.[20,41] For $n = 112-118$, this agrees with the calculations of Yoshida et al.[57] No fullerenes with 136 or 138 atoms have been described in the literature. Like our previous results for $n = 120$, 130, and 140,[20] the tails on the fullerene peaks that extend to longer drift times correspond to the tubular cages, the relative abundance of which decreases with increasing aspect ratio. Under high laser power, these elongated geometries anneal into more energetically favorable near-spherical ones, and the fullerene peaks become narrower while shifting to slightly shorter drift time.

Why Only [2+2] Dimers Are Observed. AM1 energies calculated for our optimized $C_{60}\cdot C_{56}$ and $C_{60}\cdot C_{58}$ [2+2] cycloadducts vary over several eV, depending on which bond of C_{56} or C_{58} (and which isomer of C_{56}) is used for addition.[58] However, even the lowest energy geometries for $n = 116$ and 118 are some 4-5 eV higher than the quadruply bound structures in Figure 2. Numerous "peanut" and "crimped tube" isomers[44,59,60] constructed for C_{120} are also lower in energy than [2+2] $(C_{60})_2$ by up to 6 eV,[60] and they are also absent from the products of laser desorption of fullerenes.[20] The vibrational frequencies of the [2+2] and multiply bound fullerene dimers are very similar, so the entropic contributions to the free energies are not significantly different. In any case, a single-wall fullerene is substantially lower in energy than either a "peanut" or a [2+2] cycloadduct for any cluster size.

Osawa and co-workers[46] have modeled the transformation of a [2+2] $(C_{60})_2$ into a coalesced IPR cage through a series of Stone−Wales rearrangements. While this transformation can be accomplished in many different ways, the pathway for fullerene coalescence can be viewed as a progression of local minima with decreasing center to center distance. Overall, the energy decreases by over 20 eV on going from separated C_{60} fullerenes to a coalesced cage.[11,46,55] The [2+2] cycloadduct is the first stable species encountered along the coalescence pathway. The energy of this geometry is close to that of separated fullerenes,[27,61] but there are activation barriers of a couple eV for the retro [2+2] process[18,47] and for further annealing[18] along the coalescence pathway. Because these barriers are roughly equal[18] and the isomerising cluster is continually cooled by collisions with He gas at room temperature, the system can be trapped in the [2+2] geometry. However, once over the barrier associated with the scission of two hinge bonds in the [2+2] C_{60} dimer, the potential energy decreases swiftly and the internal energy released is enough to surmount other activation barriers.[46] So the system is not trapped in any of the other intermediates along the way to the coalesced fullerene. As soon as the first IPR cage is produced, the energetic gain upon each further rearrangement step drastically declines. This apparently allows the elongated "buckytubes" to be observed in the experiments.

References and Notes

(1) Yeretzian, C.; Hansen, K.; Diederich, F.; Whetten, R. L. *Nature* **1992**, *359*, 44; *Z. Phys. D* **1993**, *26*, S300.

(2) Hansen, K.; Yeretzian, C.; Whetten, R. L. *Chem. Phys. Lett.* **1994**, *218*, 462.

(3) Beck, R. D.; Weis, P.; Brauchle, G.; Kappes, M. M. *J. Chem. Phys.* **1994**, *100*, 262.

(4) Beck, R. D.; Weis, P.; Rockenberger, J.; Kappes, M. M. *J. Phys. Chem.* **1995**, *99*, 3990.

(5) Cornett, D. S.; Amster, I. J.; Duncan, M. A.; Rao, A. M.; Eklund, P. C. *J. Phys. Chem.* **1993**, *97*, 5036.

(6) Rao, A. M.; Zhou, P.; Wang, K. A.; Hager, G. T.; Holden, J. M.; Wang, Y.; Lee, W. T.; Bi, X. X.; Eklund, P. C.; Cornett, D. S.; Duncan, M. A.; Amster, I. J. *Nature* **1993**, *259*, 955.

(7) Eklund, P. C.; Rao, A. M.; Zhou, P.; Wang, Y.; Wang, K. A.; Holden, J. M.; Dresselhaus, M. S.; Dresselhaus, G. *Mol. Cryst. Liq. Cryst.* **1994**, *256*, 199.

(8) Rao, A. M.; Eklund, P. C.; Venkateswaran, U. D.; Tucker, J.; Duncan, M. A.; Bendele, G. M.; Stephens, P. W.; Hodeau, J.-L.; Marques, L.; Nunez-Reguiero, M.; Bashkin, I. O.; Ponyatovsky, E. G.; Morovsky, A. P. *Appl. Phys. A* **1997**, *64*, 231.

(9) Eklund, P. C.; Rao, A. M.; Zhou, P.; Wang, Y.; Holden, J. M. *Thin Solid Films* **1995**, *257*, 185.

(10) Takahashi, N.; Dock, H.; Matsuzawa, N.; Ata, M. *J. Appl. Phys.* **1993**, *74*, 5790.

(11) Ata, M.; Takahashi, N.; Nojima, K. *J. Phys. Chem.* **1994**, *98*, 9960. Ata, M. Private communication.

(12) Ulmer, G.; Campbell, E. E. B.; Kuhnle, R.; Busmann, H. G.; Hertel, I. V. *Chem. Phys. Lett.* **1991**, *182*, 114.

(13) Mitzner, R.; Winter, B.; Kusch, C.; Campbell, E. E. B.; Hertel, I. V. *Z Phys. D* **1996**, *37*, 89.

(14) Tast, F.; Malinowski, N.; Billas, I. M.; Heinebrodt, M.; Branz, W.; Martin, T. P. *J. Chem. Phys.* **1997**, *107*, 6980.

(15) Rao, A. M.; Menon, M.; Wang, K. A.; Eklund, P. C.; Subbaswamy, K. R.; Cornett, D. S.; Duncan, M. A.; Amster, I. J. *Chem. Phys. Lett.* **1994**, *224*, 106.

(16) Menon, M.; Rao, A. M.; Subbaswamy, K. R.; Eklund, P. C. *Phys. Rev. B* **1995**, *51*, 800.

(17) Ata, M.; Kurihara, K.; Takahashi, N. *J. Phys. Chem. B* **1997**, *101*, 5.

(18) Hunter, J. M.; Fye, J. L.; Boivin, N. M.; Jarrold, M. F. *J. Phys. Chem.* **1994**, *98*, 7440.

(19) Dugourd, Ph.; Hudgins, R. R.; Clemmer, D. E.; Jarrold, M. F. *Rev. Sci. Instrum.* **1997**, *68*, 1122.

(20) Shvartsburg, A. A.; Hudgins, R. R.; Dugourd, Ph.; Jarrold, M. F. *J. Phys. Chem. A* **1997**, *101*, 1684.

(21) Osawa, S.; Sakai, M.; Osawa, E. *J. Phys. Chem. A* **1997**, *101*, 1378.

(22) Porezag, D.; Jungnickel, G.; Frauenheim, T.; Seifert, G.; Ayuela, A.; Pederson, M. R. *Appl. Phys. A* **1997**, *64*, 321.

(23) Fagerstrom, J.; Stafstrom, S. *Synth. Met.* **1997**, *86*, 2393. Stafstrom, S.; Fagerstrom, J. *Appl. Phys. A* **1997**, *64*, 307.

(24) Choi, C. H.; Kertesz, M. *Chem. Phys. Lett.* **1998**, *282*, 318.

(25) Esfarjani, K.; Hashi, Y.; Onoe, J.; Takeuchi, K.; Kawazoe, Y. *Phys. Rev. B* **1998**, *57*, 223.

(26) Ozaki, T.; Iwasa, Y.; Mitani, T. *Chem. Phys. Lett.* **1998**, *285*, 289.

(27) Patchkovskii, S.; Thiel, W. *J. Am. Chem. Soc.* **1998**, *120*, 556.

(28) Onoe, J.; Nakao, A.; Takeuchi, K. *Phys. Rev. B* **1997**, *55*, 10051.

(29) Onoe, J.; Takeuchi, K. *Phys. Rev. Lett.* **1997**, *79*, 2987.

(30) Agafonov, V.; Davydov, V. A.; Kashevarova, L. S.; Rakhmanina, A. V.; Kahn-Harari, A.; Dubois, P.; Ceolin, R.; Szwarc, H. *Chem. Phys. Lett.* **1997**, *267*, 193.

(31) Davydov, V. A.; Kashevarova, L. S.; Rakhmanina, A. V.; Agafonov, V.; Ceolin, R.; Szwarc, H. *Carbon* **1997**, *35*, 735.

(32) Maniwa, Y.; Sato, M.; Kume, K.; Kozlov, M. E.; Tokumoto, M. *Carbon* **1996**, *34*, 1287. Kozlov, M. E.; Tokumoto, M.; Yakushi, K. *Appl. Phys. A* **1997**, *64*, 241.

(33) Bormann, D.; Sauvajol, J. L.; Goze, C.; Rachdi, F.; Moreac, A.; Girard, A.; Forro, L.; Chauvet, O. *Phys. Rev. B* **1996**, *54*, 14139.

(34) Sauvajol, J. L.; Bormann, D.; Brocard, F.; Palpacuer, M.; Goze, C.; Rachdi, F.; Moreac, A.; Girard, A.; Forro, L.; Chauvet, O. *Synth. Met.* **1997**, *86*, 2325.

(35) Kamaras, K.; Iwasa, Y.; Forro, L. *Phys. Rev. B* **1997**, *55*, 10999.

(36) Persson, P. A.; Edlund, U.; Jacobsson, P.; Johnels, D.; Soldatov, A.; Sundqvist, B. *Chem. Phys. Lett.* **1996**, *258*, 540.

(37) Winter, J.; Kuzmany, H.; Soldatov, A.; Persson, P. A.; Jacobsson, P.; Sundqvist, B. *Phys. Rev. B* **1996**, *54*, 17486.

(38) Wagberg, T.; Persson, P. A.; Sundqvist, B.; Jacobsson, P. *Appl. Phys. A* **1997**, *64*, 223.

(39) Burger, B.; Winter, J.; Kuzmany, H. *Z. Phys. B* **1996**, *101*, 227. Kuzmany, H.; Winter, J.; Burger, B. *Synth. Met.* **1997**, *85*, 1173. Burger, B.; Winter, J.; Kuzmany, H. *Synth. Met.* **1997**, *86*, 2329.

(40) Venkateswaran, U. D.; Sanzi, D.; Krishnappa, J.; Marques, L.; Hodeau, J. L.; Nunez-Reguero, M.; Rao, A. M.; Eklund, P. C. *Phys. Status Solidi b* **1996**, *198*, 545.

(41) Shvartsburg, A. A.; Schatz, G. C.; Jarrold, M. F. *J. Chem. Phys.* **1998**, *108*, 2416.

(42) Wang, G. W.; Komatsu, K.; Murata, Y.; Shiro, M. *Nature* **1997**, *387*, 583.

(43) Lebedkin, S.; Gromov, A.; Giesa, S.; Gleiter, R.; Renker, B.; Rietschel, H.; Kratschmer, W. *Chem. Phys. Lett.* **1998**, *285*, 210.

(44) Osawa, S.; Osawa, E.; Hirose, Y. *Fullerene Sci. Technol.* **1995**, *3*, 565.

(45) Honda, K.; Osawa, E.; Slanina, Z.; Matsumoto, T. *Fullerene Sci. Technol.* **1996**, *4*, 819.

(46) Ueno, H.; Osawa, S.; Osawa, E.; Takeuchi, K. *Fullerene Sci. Technol.* **1998**, *6*, 319.

(47) Wang, Y.; Holden, J. M.; Bi, X. X.; Eklund, P. C. *Chem. Phys. Lett.* **1994**, *217*, 413.

(48) Haufler, R. E.; Wang, L. S.; Chibante, L. P. F.; Jin, C.; Conceicao, J.; Chai, Y.; Smalley, R.E. *Chem. Phys. Lett.* **1991**, *179*, 449.

(49) Petrie, S.; Bohme, D. K. *Nature* **1993**, *356*, 426.

(50) Mason, E. A.; McDaniel, E. W. *Transport Properties of Ions in Gases*; Wiley: New York, 1988.

(51) Mesleh, M. F.; Hunter, J. M.; Shvartsburg, A. A.; Schatz, G. C.; Jarrold, M. F. *J. Phys. Chem.* **1996**, *100*, 16082; *J. Phys. Chem. A* **1997**, *101*, 968.

(52) Shvartsburg, A. A.; Jarrold, M. F. *Chem. Phys. Lett.* **1996**, *261*, 86.

(53) Stanton, R. E. *J. Phys. Chem.* **1992**, *96*, 111.

(54) Zhang, B. L.; Wang, C. Z.; Ho, K. M.; Xu, C. H.; Chan, C. T. *J. Chem. Phys.* **1992**, *97*, 5007.

(55) Eckhoff, W. C.; Scuseria, G. E. *Chem. Phys. Lett.* **1993**, *216*, 399. Murry, R. L.; Strout, D. L.; Scuseria, G. E. *Int. J. Mass Spectrom. Ion Processes* **1994**, *138*, 113.

(56) Hunter, J. M.; Jarrold, M. F. *J. Am. Chem. Soc.* **1995**, *117*, 10317.

(57) Yoshida, M.; Goto, H.; Hirose, Y.; Zhao, X.; Osawa, E. *Electron J. Theor. Chem.* **1996**, *1*, 163.

(58) Pederson, L. A.; Schatz, G. C. Unpublished results.

(59) Strout, D. L.; Murry, R. L.; Xu, C.; Eckhoff, W. C.; Odom, G. K.; Scuseria, G. E. *Chem. Phys. Lett.* **1993**, *214*, 576.

(60) Galpern, E. G.; Stankevich, I. V.; Chistyakov, A. L.; Chernoza-tonskii, L. A. *Chem. Phys. Lett.* **1997**, *269*, 85.

(61) Scuseria, G. E. *Chem. Phys. Lett.* **1996**, *257*, 583.